Photo-Luminescence Modulation Circuits for Solar Cell Based Optical Communications

Walter D. Leon-Salas School of Engineering Technology Purdue University Xiaozhe Fan School of Engineering Technology Purdue University

Abstract—High-efficiency solar cells, such as GaAs solar cells, exhibit strong luminescent emissions in the infrared. This paper presents two circuits that are able to modulate these luminescent emissions while harvesting energy from the solar cell. These circuits can be used in Internet-of-Things applications where devices need an energy source and a means to transmit information wirelessly. The proposed circuits are based on a boost DC-DC converter and are suitable for binary (on-off) modulation. These circuits require only minimal additional hardware (either a switch or an AND gate) for their implementation. Proof-of-concept prototypes of these circuits were built and tested. Experimental results show a tradeoff between harvested energy and bit error rate.

I. INTRODUCTION

The Internet-of-Things is a vision in which the Internet seamlessly extends to objects around us. In this vision, objects such as appliances, furniture and machines connect to the Internet to exchange information about themselves and their surroundings in order to monitor, control and overall enhance our environment [1].

Wireless communications and energy harvesting (EH) are key enabling technologies for the IoT. Wireless communications enable easy integration of IoT devices with everyday objects while EH avoids manual battery recharging or replacement. Radio-based communication has been the dominant wireless technology for establishing connectivity between IoT devices. Most IoT solutions use unlicensed radio bands to ease adoption. The IoT market has been experiencing rapid growth and it is expected that by 2020, 24 billion devices will be connected to the Internet [2]. As more and more IoT devices are deployed, unlicensed bands will become increasingly crowded slowing down transmission speeds and increasing mutual interference. In some places, such as hospitals and airplanes, radio transmissions are discouraged altogether to avoid interference with sensitive medical and navigation equipment.

Energy can be harvested from different ambient sources such as light, heat, motion, radio-frequency fields and vibrations. Among all these sources of ambient energy, light or radiant energy is the most available source of energy both for indoors and outdoors scenarios with power densities ranging from 100 mW/cm² for outdoors to 0.1 mW/cm² for well-lit indoors spaces [3]. In contrast, the average power densities for mechanical and RF energy are 8.6 μ W/cm² and 6 μ W/cm², respectively [9,10]. Moreover, the technology for harvesting

light energy also scales well for micro [4,5], meso [6,7] and macro-scale [8] devices.

Recently, an optical communication scheme that employs solar cells as optical antennas to transmit and receive information wirelessly while harvesting radiant energy was reported in [11] and expanded in [12]. In this scheme, the luminescent emissions of high-efficiency solar cells, such as GaAs cells, are modulated with information. The solar cell, by virtue of its photo-transduction property, also works as an optical receiver [13,14]. This communication approach has been dubbed Optical Frequency Identification (OFID) for its analogy with Radio Frequency Identification (RFID). Some of the advantages of OFID include the possibility of using cameras to receive and spatially locate optical transmissions, communications free of electromagnetic interference, the unregulated nature of the optical portion of the electromagnetic spectrum, the possibility of mounting optical transmitters or receivers on metallic surfaces without detuning and the possibility for underwater communications. The main drawback of OFID is its need for line of sight. This drawback, however, could be exploited to secure wireless communication links against eavesdropping. Potential applications of OFID include: smart labels, environmental sensors, smart home monitoring, underwater markers and tags for locating and tracking of people or goods in hospitals, factories or at home.

The work in [12] presented a photo-luminescence modulation circuit based on a boost DC-DC converter. This circuit was able to modulate the photo-luminescent output of a solar cell while harvesting energy from the solar cell. It employed a pulse width modulator and an analog multiplexer to vary the duty cycle of the DC-DC converter according to the data symbols being transmitted. Although this circuit had the capability for multi-level modulation, the spacing between modulation levels was non-linear and it was a function of light intensity. As a result, the modulation levels had to be constantly updated. Here, two low-complexity photoluminescence modulation circuits for solar cells are presented. The modulation circuits are suitable for On-Off Keying (OOK) modulation and require either an AND gate or a switch for their hardware implementation. These modulators are based on a boost DC-DC converter. Hence, they are able to harvest energy while transmitting information.

The rest of this paper is organized as follows: Section II presents a brief introduction to luminescence in solar cells and

OFID technology, section III describes the proposed modulators, section IV presents experimental results and section V concludes the paper.

II. BACKGROUND

The emission of photons from an excited material is called luminescence. If the material is excited by light, this emission is called photo-luminescence (PL). Solar cell materials exhibit different degrees of luminescence. Silicon for instance, has very weak luminescence due to its indirect bandgap electronic structure. However, solar cells made out of direct bandgap semiconductor materials, such as GaAs, have strong luminescent emissions. For GaAs solar cells these PL emissions are in the infrared (IR) part of the electro-magnetic spectrum (\sim 870 nm).

The luminescent radiant flux of a solar cell, Φ_{lum} , is a function of the voltage across the solar cell. Thus, it can be modulated by varying the solar cell voltage [12]. A circuit model for a solar cell that includes Φ_{lum} was presented in [12]. In this model, the diode that is typically used to model the non-linear behavior of a solar cell is replaced with a light-emitting diode (LED) as shown in Fig. 1.

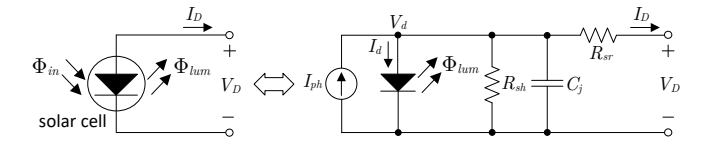


Fig. 1: Circuit model of a solar cell including emitted luminescent radiation Φ_{lum} . An LED is used to model the solar cell and to account for the luminescent output.

The following expression for Φ_{lum} was also derived in [12]:

$$\Phi_{lum} = \eta \kappa R \left(QE(\lambda_i) \Phi_{in} - \frac{E_{ph}^e I_s}{q} + \frac{E_{ph}^e I_s e^{V_D/nV_T}}{q} \right)$$
(1)

where, η is the fraction of photons generated inside the solar cell that escape the solar cell, κ is the fraction of the recombined electrons that recombine radiatively, R is the fraction of the photo-generated electrons that recombine inside the solar cell and do not contribute to the solar cell current, $QE(\lambda_i)$ is the quantum efficiency at the wavelength of the incident light λ_i , Φ_{in} is the incident radiant flux, E^e_{ph} is the energy of an emitted photon, I_s is the reverse saturation current of the LED, q is the electron's charge, V_D is the voltage across the solar cell, V_T is the thermal voltage and n is the diode's ideality factor. In this model the series resistance of the solar cell R_{sr} is assumed to be close to zero $(V_d \approx V_D)$. Fig. 2 shows a plot of the Φ_{lum} vs V_D relationship given in (1) for $\lambda_i = 623$ nm, $\eta = 0.4$, $\kappa = 0.8$, R = 0.1, $QE(\lambda_i) = 0.8$, $E^e_{nh} = 1.4$ eV, $\Phi_{in} = 1.5$ mW and $nV_T = 30$ mV.

For EH purposes the solar cell must operate in the photovoltaic region, $0 < V_D < V_{oc}$, where it generates power. Outside this region the solar cell dissipates power. V_{oc} is the open circuit (OC) voltage of the solar cell.

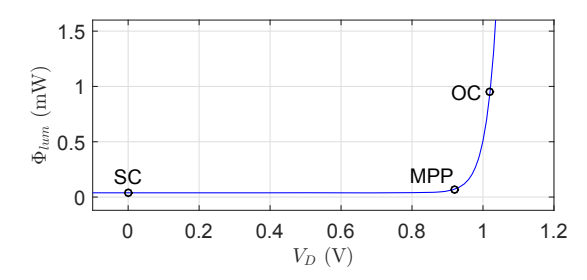


Fig. 2: Plot of the Φ_{lum} vs V_D relationship. The SC, MPP and OC operating points of the solar cell are marked.

On the plot of Fig. 2, the following operating points of the solar cell have been marked: Short Circuit (SC), Maximum Power Point (MPP) and OC. Among these three operating points, the luminescent radiant flux at SC (Φ_{lum}^{sc}) is the lowest and it is the highest at OC (Φ_{lum}^{oc}). At the MPP, the luminescent radiant flux is Φ_{lum}^{mpp} . In terms of EH, the solar cell generates maximum power at the MPP. At the SC or OC operating points the solar cell generates zero power.

In the OFID concept, the relationship between Φ_{lum} and V_D is exploited to modulate the luminescent emissions of a solar cell to build wireless devices that communicate optically using their on-board solar cells and harvest radiant energy from their environment to power themselves up or to recharge an energy reservoir such as a battery or a super-capacitor. Fig. 3 depicts a conceptual diagram of an OFID communication system. The main components of an OFID system are a reader and an OFID device. The solar cell of the OFID device works as an optical transmitter when its luminescent emissions are modulated with information. The solar cell also works as a photo-detector to receive information encoded optically by the reader and as an energy harvester.

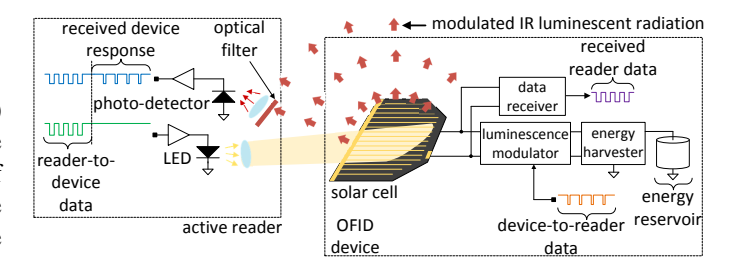


Fig. 3: Conceptual diagram of the OFID communication scheme.

Fig. 3 shows an active reader, that is, a reader that generates its own light to actively illuminate the solar cell of an OFID device. A passive reader is also possible. A passive reader does not actively illuminate a solar cell but relies on ambient light, such as sun light, to stimulate a PL response from the solar cell.

The main components of an OFID device are a solar cell, a luminescence modulator, a data receiver, an energy harvester and an energy reservoir. This work focuses on the luminescence modulator. Two low-complexity PL modulators for OOK modulation are presented in the next section.

III. PHOTO-LUMINESCENCE MODULATORS

The modulator circuits presented in this work are based on a boost DC-DC converter. The boost DC-DC converter is used to harvest energy by transferring electrical charges from the solar cell to a load, which could be an electronic circuit or an energy reservoir, while boosting the relatively low voltage of a solar cell ($\sim 1.0~\rm V$ for GaAs solar cells) to a voltage that is compatible with most electronic circuits. Hence, the proposed modulator circuits are able to harvest energy while transmitting information.

Fig. 4 shows the first modulator and EH circuit (Circuit 1) while Fig. 5 shows the second modulator circuit (Circuit 2). In these figures, d_{in} is the binary data being transmitted.

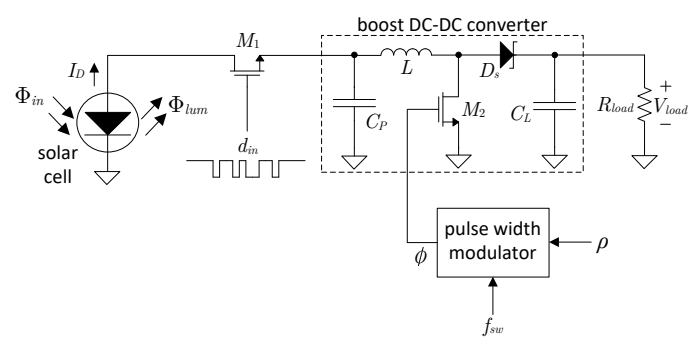


Fig. 4: Circuit 1. This modulator employs a MOSFET in front of a DC-DC converter. The MOSFET works as a switch connecting and disconnecting the DC-DC converter from the solar cell according to the data being transmitted d_{in} .

Both circuits use a pulse width modulator to generate a clock signal ϕ of frequency f_{sw} that drives the gate of transistor M_2 . The duty cycle ρ of this clock signal is adjusted until the maximum power is delivered to the load. At that point the DC-DC converter is said to be operating at the MPP. The location of the MPP changes with the incident radiant flux (Φ_{in}) . Hence, ρ needs to be constantly updated to ensure that maximum power is always being drawn from the solar cell. This is the work of an MPP controller. Several MPP controllers have been proposed in the literature [15]. Here, we assume that an MPP controller is available and that the DC-DC converter is working at the MPP.

Circuit 1 employs a metal oxide semiconductor field effect transistor (MOSFET) M_1 in between the solar cell and the DC-DC converter. The MOSFET works as a switch connecting and disconnecting the DC-DC converter from the solar cell according to d_{in} . When d_{in} is logic high (1), M_1 conducts connecting the solar cell to the DC-DC converter. Since the DC-DC converter is working at the MPP, connecting it to the solar cell biases the solar cell at the MPP causing it to emit a radiant flux of Φ_{lum}^{mpp} . When d_{in} is logic low (0), the solar cell gets disconnected from the DC-DC converter leaving the solar cell in OC. Hence, for $d_{in} = 0$, the solar cell emits a radiant flux of Φ_{lum}^{oc} . When data is not being transmitted, d_{in} remains at logic high allowing the DC-DC converter to harvest energy.

Circuit 2 employs an AND logic gate to modulate the clock signal ϕ with the data d_{in} . When $d_{in}=1$, the AND gate outputs the clock signal ϕ , which sets the operating point of the solar cell to the MPP. Thus, when $d_{in}=1$ the solar cell emits Φ_{lum}^{mpp} .

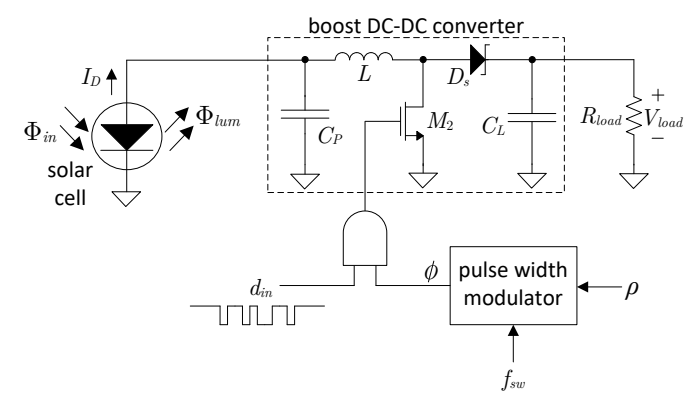


Fig. 5: Circuit 2. This modulator employs an AND gate to modulate the clock signal ϕ that drives the DC-DC converter with the data being transmitted d_{in} .

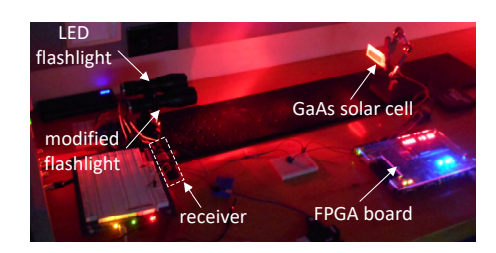
When $d_{in}=\mathbf{0}$, the AND gate outputs a $\mathbf{0}$, which turns off M_2 and prevents inductor L from recharging. As a consequence, capacitor C_P gets charged to V_{oc} by the solar cell. Thus, when $d_{in}=\mathbf{0}$ the solar cell operates at the OC and emits Φ_{lum}^{oc} . The data bit rate for both circuits is limited to values below f_{sw} .

IV. EXPERIMENTAL RESULTS

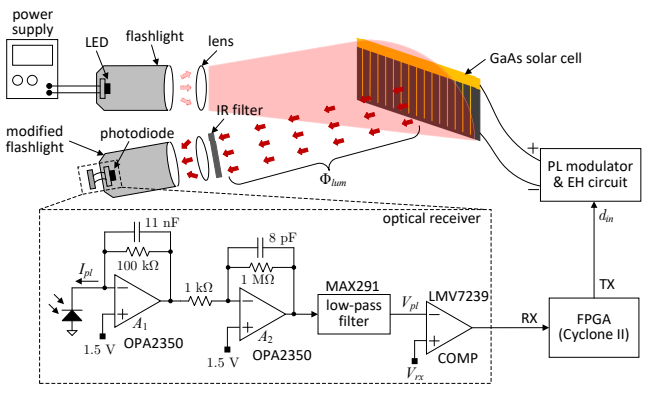
Fig. 6 shows the test setup that was built to assess the performance of the PL modulation and EH circuits. The setup consists of an LED flashlight with light emission centered at 623 nm, a GaAs solar cell, a PL modulator & EH circuit, a field programmable gate array (FPGA) and an optical receiver. The optical receiver comprises a photo-diode, two amplifiers $(A_1 \text{ and } A_2)$, an 8th order low-pass filter (MAX291) and a comparator (COMP). The photo-diode was housed in a modified flashlight with adjustable focus. An 850 nm long-pass IR filter was placed in front of this flashlight. The low-pass filter removes the ripple noise generated by the switching action of the DC-DC converter. The amplifiers in the optical receiver provide a trans-impedance gain of $10^8 \Omega$. Together the optical receiver and the LED flashlight form the OFID reader.

Fig. 7 shows key waveforms recorded from Circuit 1 (V_{out} , d_{in} and V_d) and from the reader (V_{pl}). Likewise, Fig. 8 shows these waveforms for Circuit 2. In both cases the waveforms were recorded at a distance d=51 cm between the solar cell and the reader and when d_{in} is an alternating sequence of 1s and 0s at a rate of 5 kbps. The following parameters were used for both circuits: $f_{sw}=40$ kHz, $R_{load}=5.1$ k Ω , $C_P=1$ μ F, L=68 μ H and $C_L=10$ μ F. The measured optical power emitted by the LED flashlight was measured to be 11.04 mW.

Notably, Circuit 2 is able to harvest more power from the solar cell (generates a higher output voltage V_{out}) than Circuit



(a) Photograph of the test setup.



(b) Schematic diagram of the test setup.

Fig. 6: Test setup built to assess the performance of the PL modulation and EH circuits.

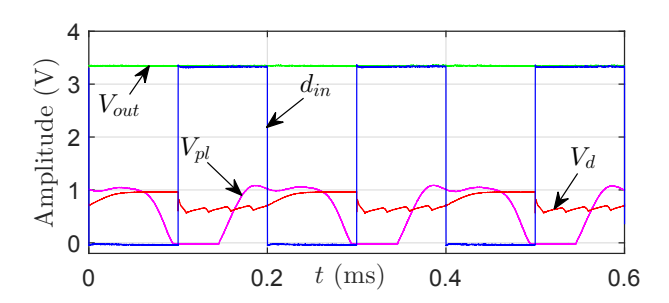


Fig. 7: Waveforms recorded from Circuit 1 and the reader.

1. Circuit 2 has a better EH performance because, even when a ${\bf 0}$ is transmitted, the solar cell never gets fully disconnected from the DC-DC converter. As a consequence, the solar cell continues to charge capacitor C_P even when $d_{in}={\bf 0}$. On the other hand, for Circuit 1, the voltage across the solar cell, V_d , exhibits a larger signal swing as d_{in} changes. This larger signal swing is due to the fact that C_P gets fully disconnected from the solar cell when $d_{in}={\bf 0}$. A larger swing in V_d translates into a larger swing in Φ_{lum} and as a consequence into a higher signal-to-noise ratio (SNR) at the receiver.

To further illustrate the EH and SNR qualities of Circuits 1 and 2, the harvested power P_{load} and the bit error rate (BER) were measured for both circuits as the distance d varied from 12 cm to 70 cm. The FPGA was used to generate a sequence of pseudo-random bits at a rate of 15 kbps. Figs. 9 and 10 show the results of these measurements. As it can be seen from these figures, Circuit 2 delivers more power to the load

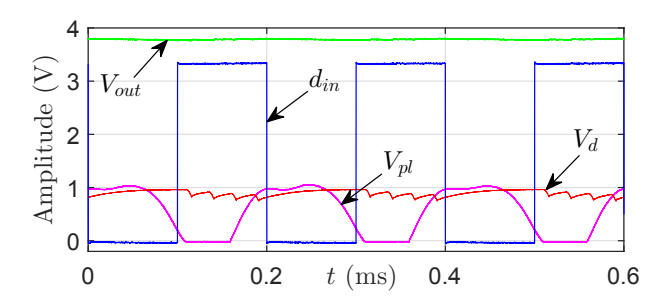


Fig. 8: Waveforms recorded from Circuit 2 and the reader.

than Circuit 1 does at any distance. However, the BER starts to rise sharply at d=61 cm for Circuit 2 and at d=66 cm for Circuit 1. Hence, slightly longer communication distances can be achieved with Circuit 1.

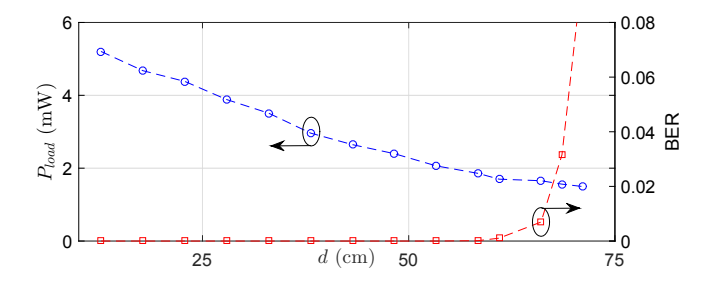


Fig. 9: Harvested power (P_{load}) and BER performance for Circuit 1 as a function of distance d.

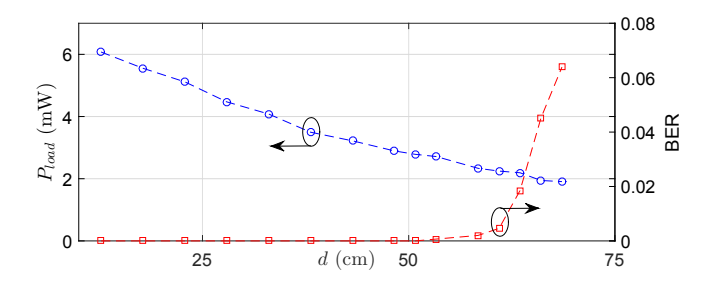


Fig. 10: Harvested power (P_{load}) and BER performance for Circuit 2 as a function of distance d.

V. CONCLUSION

Two circuits that are able to modulate the luminescent emissions of solar cells while harvesting energy from the solar cell are presented. Both circuits are based on a boost DC-DC converter and are suitable for the transmission of binary (on-off) information. The proposed circuits have low hardware complexity. They require either a transistor working as a switch of an AND gate. Experimental results show that there is a tradeoff between harvested power and bit error rate. The modulator circuit based on the switch achieves the best bit error rate performance while the modulator circuit based on the AND gate achieves the best energy harvesting performance.

ACKNOWLEDGMENT

The authors would like to thank the National Science Foundation for its support through grant ECCS-1809637.

REFERENCES

- A. Al-Fuaqba, M. Guizani, M. Mohammadi, M. Aledhari and M. Ayyash, "Internet of things: a survey on enabling technologies, protocols and applications, *IEEE Communication Surveys and Tutorials*, vol. 17, no. 4, pp. 2347-2376, 2015.
- [2] J. Gubbi, R. Buyya, S. Marusic and M. Palaniswami, "Internet of Things (IoT): a vision, architectural elements and future directions, *Future Generation Computing Systems*, vol. 29, p. 1645-1660, 2013.
- [3] M. Gorlatova, P. Kinget, I. Kymissis, D. Rubenstein, X. Wang and G. Zussman, "Energy harvesting active networked tags (EnHANTs) for ubiquitous object networking, *IEEE Wireless Communications*, vol. 17, no. 6, pp. 18-25, 2010.
- [4] B. A. Warneke, M. Last, B. Liebowitz and K. S. J. Pister, "Smart dust: communicating with a cubic-millimeter computer," *Computer*, vol. 34, no, 1, pp. 44-51, 2001.
- [5] G. Moayeri Pour, M. K. Benyhesan and W. D. Leon-Salas, "Energy harvesting using substrate photodiodes," *IEEE Trans. on Circuits and Systems-II*, vol. 61, on. 7, pp. 501-505, 2014.
- [6] C.-T. Lee et al, "EcoMicro: a miniature self-powered inertial sensor node based on Bluetooth low energy,"
- [7] H.-T. Wang and W. D. Leon-Salas, "An image sensor with joint sensing and energy harvesting functions," *IEEE Sensors Journal*, vol. 15, no. 2, pp. 902-916, 2015.
- [8] C. Alippi, R. Camplani, C. Galperti and M. Roveri, "A robust, adaptive, solar-powered WSN framework for aquatic environmental monitoring," *IEEE Sensors Journal*, vol. 11, no. 1, pp. 45-55, 2011.
- [9] M. Gortalova, J. Sarik, G. Grebla, M, Cong, I. Kymissis and G. Zussman, "Movers and shakers: kinetic energy for the internet of things, *IEEE Journal on Selected Areas in Communications*, vol. 33, no. 8, pp. 1624-1638, 2015.
- [10] M. Pinuela, P. D. Mitcheson and S. Lucyszyn, "Ambient RF energy harvesting in urban and semi-urban environments," *IEEE Trans. on Microwave Theory and Techniques*, vol. 61, no. 7, pp. 2715-2726, 2013.
- [11] W. D. Leon-Salas and X. Fan, "Exploiting luminescence emissions of solar cells for optical frequency identification," *IEEE International Symposium on Circuits and Systems (ISCAS)*, Florence, May 2018.
- [12] W. D. Leon-Salas and X. Fan, "Solar cell photo-luminescence modulation for Optical Frequency Identification Devices," *IEEE Trans. on Circuits and Systems-I*, pp. 1-12, Sept. 2018.
- [13] Z. Wang, D. Tsonev, S. Videv and H. Haas, "On the design of a solar-panel receiver for optical wireless communications with simultaneous energy harvesting," *IEEE Journal on Selected Areas in Communications*, vol. 33, no. 8, pp. 1612-1623, 2015.
- [14] X. Fan and W. D. Leon-Salas, "A circuit for simultaneous optical data reception and energy harvesting," *IEEE Int. Midwest Symposium* on Circuits and Systems, Oct. 2017.
- [15] M. A. Gomes de Brito, L. Galotto, L. P. Sampaio, G. de Azevedo e Melo and C. A. Canesin, "Evaluation of the main MPPT techniques for photovoltaic applications," *IEEE Trans. on Industrial Electronics*, vol. 60, no. 3, pp. 1156-1167, 2013.